Applied Physics Letters ARTICLE scitation.org/journal/apl

Nitrogen in silicon for room temperature single-electron tunneling devices

Cite as: Appl. Phys. Lett. **122**, 083502 (2023); doi: 10.1063/5.0136182
Submitted: 24 November 2022 · Accepted: 6 February 2023 ·
Published Online: 21 February 2023

Pooja Yadav,[1] Hemant Arora,[1] and Arup Samanta[1,2,a)]

AFFILIATIONS

[1]Department of Physics, Indian Institute of Technology Roorkee, Roorkee 247667, Uttarakhand, India
[2]Centre of Nanotechnology, Indian Institute of Technology Roorkee, Roorkee 247667, Uttarakhand, India

[a)]Author to whom correspondence should be addressed: arup.samanta@ph.iitr.ac.in

ABSTRACT

Single-electron transistor (SET) has an advanced feature that can be exploited in quantum devices. For practical utilization of such devices, the room-temperature operation is highly essential. Dopant-based single-electron devices are well studied at low temperatures although a few devices are developed for high-temperature operation with certain limitations. Here, we propose and theoretically exhibit that nitrogen (N) donor in silicon is an important candidate for the effective designing of quantum devices. Theoretical calculation of the density of states using the semi-empirical density functional theory method indicates that N-donor in silicon has a deep ground state compared to a phosphorus (P) donor. The N-donor spectrum is explored in nano-silicon structure along with the P-donor. A comparative study of the Bohr radius of N-donor and P-donor is also reported. The simulated current–voltage characteristics confirm that the N-doped device is better suited for SET operation at room temperature.

In the past two decades, a significant effort had been put into developing single-electron tunneling devices using dopant atoms for solid state-based quantum architecture by utilizing and manipulating the charge and spin degrees of freedom using external fields.[1–4] Dopant-based single-electron transistor (SET) devices are key components in quantum device applications, e.g., quantum bit,[1] memory,[5] single-electron pump,[6] single charge sensing,[7] and single photon detectors.[8] Extensive research work has been carried out on a few dopant-based devices, where single-electron tunneling effect is observed at low temperatures.[9–14] However, the operation of such devices at room temperature is highly needed for practical utilization. The reason is the low barrier height and low charging energy due to the shallow nature of dopants, e.g., arsenic (As) and phosphorous (P) as donors and boron (B) as an acceptor in silicon. Some results of these devices at high operational temperatures have also been reported using quantum confinement, dielectric confinement, and multi-donor cluster.[15,16]

To improve the operating temperature of such SET devices, alternative dopants are also proposed for the utilization of double donors like tellurium (Te), selenium (Se), and sulfur (S), which have one order higher binding energy than shallow donors.[17] Recently, the spin relaxation and donor–acceptor recombination of Se^+ in ^{28}Si was reported.[18] However, the use of double donors needs control of several associated effects due to the existence of multiple electrons in the donor. Erbium being a deep donor has also been studied for spin-based devices.[19] High-temperature operation of the germanium-vacancy complexes-based devices has recently been proposed and demonstrated.[20,21] Room-temperature operation of the deep donor pair of Al–N in silicon is reported in tunnel field effect transistor (TFET) configuration.[22] However, the use of a single deep dopant is better for quantum operation due to the minimization of decoherent path.

Here, we propose an alternative quantum architecture for such approach using nitrogen (N) donor in FinFET/SOI-FET configuration for high-temperature operation and also explore the N-donor spectrum in bulk-silicon, nano-silicon, and in device configuration. The well-known ground state (GS) energy of the nitrogen from the conduction band of bulk silicon is ∼190 meV.[23] Due to this high binding energy, nitrogen in silicon can be a suitable candidate for high temperature single-electron tunneling devices. This means the discrete states of N-donor can be preserved at room temperature by suppressing the crosstalk with the external environment and saving the electron states from thermal demons. Taking into account the natural abundance of ^{28}Si isotope as a host medium and the deep donor energy level of nitrogen donor, both electronic and spin states can also be conserved for a longer time.[24] In addition, this system could also be an important candidate for nuclear spin qubit by analogy with the P-donor in

silicon, since the N-donor has multiple values of isotopic nuclear spin compared to zero isotopic spin of the host medium.[1]

In this Letter, we design the undoped, phosphorous doped, and nitrogen doped hydrogenated silicon nanowire (H:SiNW) along with the bulk structure in normal and SET configurations and perform the comparative analyses using the semi-empirical density functional theory (DFT) for these configurations. The projected density of states (PDOS), the total density of states (TDOS), and the local density of states (LDOS) along with the current–voltage (I_{DS}–V_G) characteristics are studied. Single-electron tunneling transport through the discrete energy states of donors is investigated for both P-doped and N-doped devices at low and room temperatures.

The numerical calculations are performed using the Quantum ATK software[25] based on density functional theory. The semi-empirical extended-Hückel[26] method is used for these calculations at 300 K. The mesh cutoff is set at 20 Hartree. The k grid $1 \times 1 \times 174$ is used. The atomistic structure of a silicon nanowire of length 32.4 Å and diameter 10 Å is constructed along [100] direction. The surface dangling bonds are passivated by the hydrogen atoms. The schematic and atomistic design of different structures are presented in Figs. 1(a) and 1(b). An inbuilt optimizer is utilized for structure optimization with force constant 0.008 eV^{-1}. This structure is used to calculate the TDOS and PDOS spectra of H:SiNW. In addition, we examined the density of states profile of undoped, P-doped, and N-doped bulk silicon used with $4 \times 4 \times 4$ fcc supercell (512 Si lattice sites). The density mesh cutoff is set to 20 Hartree with $4 \times 4 \times 4$ k-point set proposed by Makov *et al.*[27]

To study donor-based transistor devices, the SiNW transistors, having a diameter of 10 Å and a length of 54 Å, are also structured by gate-all-around assembly along with tunnel coupling of the center dopant with source and drain reservoirs as shown in Fig. 1(c). In these devices, the gate covers the channel region of the donor's location of the SET devices. The vacuum is used as a gate dielectric for the present configurations. The source and drain leads are heavily doped with n-type dopant with the concentration of 1×10^{21} cm^{-3}. The I_{DS}–V_G characteristics of these devices are calculated using the non-equilibrium Green's function (NEGF) method with Landauer formalism.[28]

Initially, the TDOS spectra of undoped, P-doped, and N-doped bulk systems are studied in Figs. 2(a)–2(c). The undoped bulk silicon shows a bandgap of 0.6 eV as presented in Fig. 2(a), consistent with previous reports.[29] The P-doped and N-doped bulk Si systems are studied subsequently. Here, the Fermi energy is set at 0 eV for all results. The donor energy state is found at $E - E_F = 0$ eV for both cases, which are the ground states of the respective donors. The separation between the ground state (GS) and next conducting state of donors depicts the shallow nature of the P-donor, while that is deep for N-donor. In the TDOS spectrum of P-donor in Fig. 2(b), the mixed states are present at $E - E_F = 0$ eV, which cannot be distinctly separated due to thermal smearing. In the TDOS spectrum of N-doped bulk silicon as shown in Fig. 2(c), the ground state and the next conducting state of the donor lie at 0 eV and 184 meV, respectively. Since the donor states are merged in the conduction band of bulk structure, it is difficult to separate donor states further. Hence, the separation of the GS of N-donor with conduction band edge (CBE) is 184 meV, consistent with the experimentally reported value.[30]

To understand the behavior of donors in nano-silicon, we investigated the same analysis for H:SiNW systems. From now onward, all the calculations are performed on H:SiNW. The TDOS spectra of undoped, P-doped, and N-doped H:SiNW are calculated and presented in Figs. 2(d)–2(f), respectively. In the TDOS spectrum of undoped H:SiNW as shown in Fig. 2(d), the separation between the conduction-band and valence-band edges is very high (~1.7 eV), indicating the increase in bandgap due to the confinement effect.

Modification in the TDOS features is observed in both P-doped and N-doped systems compared to undoped H:SiNW as presented in Figs. 2(e) and 2(f), respectively. Additional states within the bandgap are observed in doped structures. To probe the TDOS spectra in detail, the PDOS spectra are studied to identify and locate the states of the donor. It is well documented that the donor energy level in silicon splits into three energy groups due to valley degeneracy: one A_1 state (lowest energy state), one threefold T_2 state (first excited state, ES), and one twofold E state (second excited state).[31,32] The A_1 orbital shows the s-like symmetry on the dopant location of nanostructure, while the T_2 and E orbitals show a node at this position.[33] The A_1, T_2, and E states are identified for both P-donor and N-donor in this study in comparison with the literature.[34]

We focused on the position dependent PDOS of the P-donor in Figs. 3(a)–3(d). The PDOS components of s, p, and d orbitals of the P-donor on itself, i.e., $d = 0$ exhibit that A_1, T_2, and E energy levels

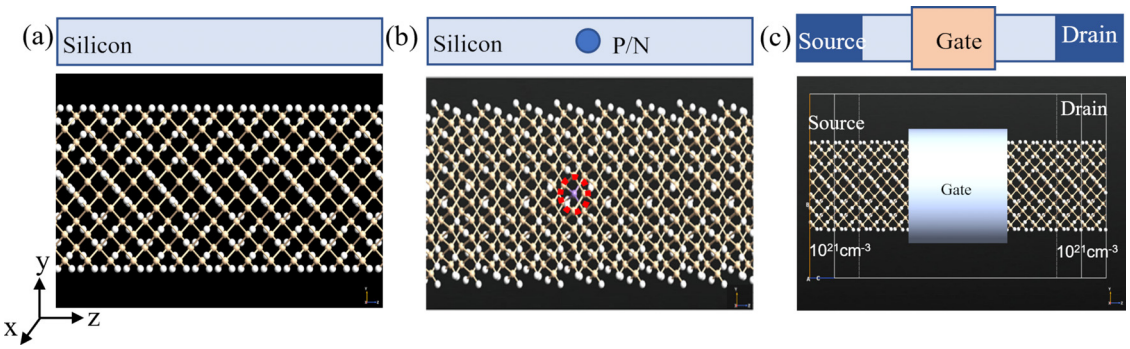

FIG. 1. (a) Quantum ATK simulated structure for (a) H:SiNW, (b) substitutional P/N-doped (encircled by the red dotted line) H:SiNW, and (c) P/N-doped H:SiNW in transistor configuration with gate terminal and source drain terminals. Top Panel: schematic design of structures for (a)–(c). SiNW radius is in x–y dimension, and z dimension is along the length axis.

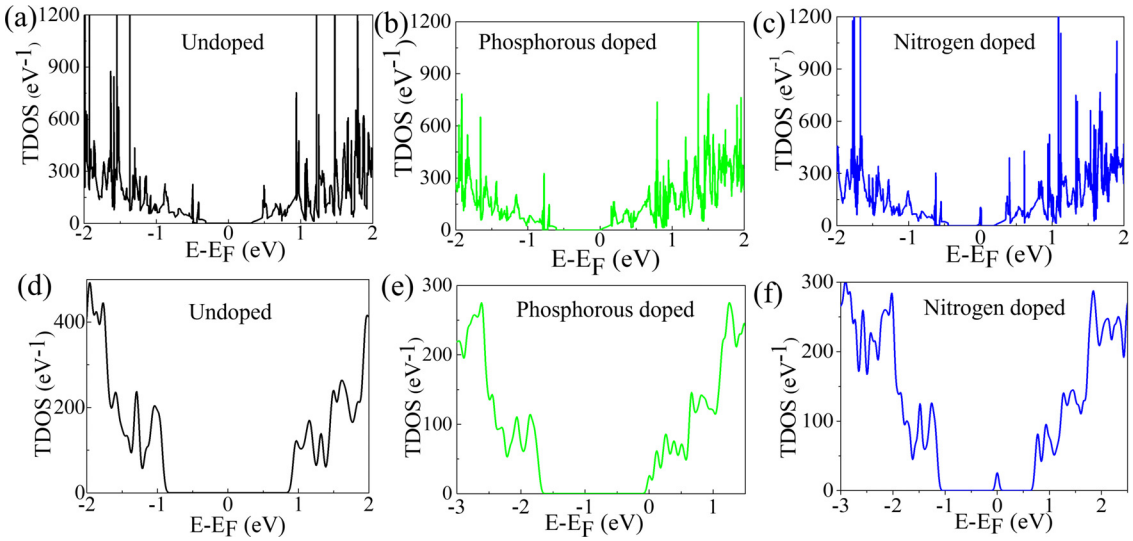

FIG. 2. (a)–(c) TDOS spectra of undoped, P-doped, and N-doped bulk silicon. (d)–(f) TDOS spectra of undoped, P-doped, and N-doped H:SiNW.

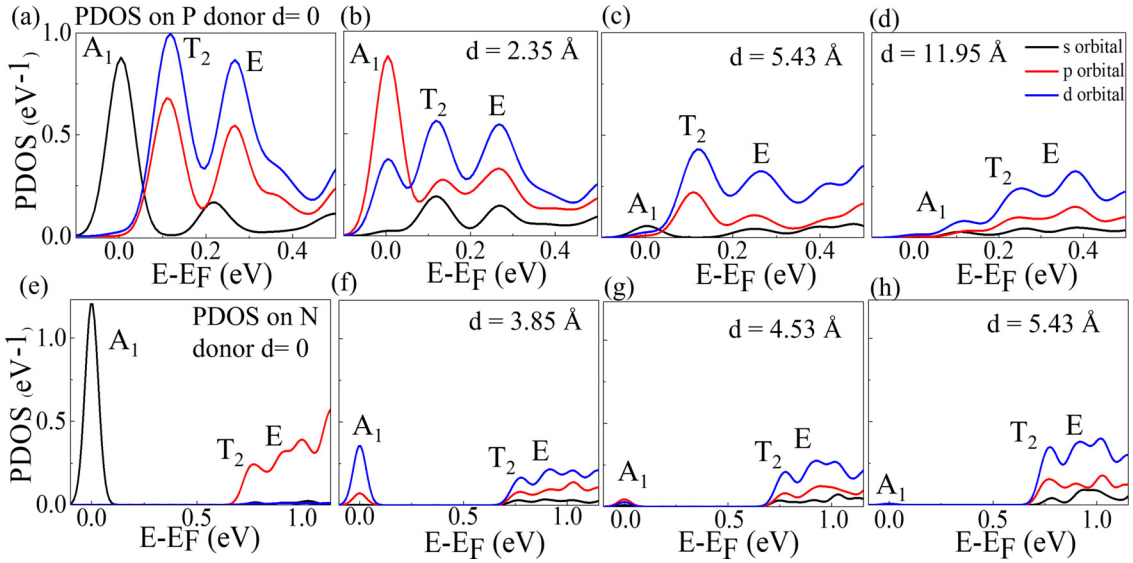

FIG. 3. (a)–(d) PDOS spectra of P-doped H:SiNW for different positions along the channel starting from the P-donor location, where the states A_1, T_2, and E are identified. (e)–(h) Same spectra for N-donor atom.

exist at this location, where A_1 state is the lowest energy state and is mainly coming from the s-orbital of the P-donor.

The T_2 and E energy levels are the mixture of s, p, and d-orbitals. The PDOS spectrum of P-donor on different silicon locations is investigated in Figs. 3(b)–3(d), where the distance parameter from the donor location toward the drain reservoir side is defined as "d." The existence of the PDOS on the silicon position confirms that the hybridization is present between the electronic states of P and Si atoms. We mainly focus on the ground state (i.e., A_1) of the P-donor, which diminishes as we move away from the donor location. The localization of the A_1 state can be correlated with the spreading of this state. Such behavior can be linked to the Bohr radius of the ground state, which is the distance from where the A_1 state originates and where the A_1 state dies out. The extinction of the A_1 state is the end of this state, and its length from the donor location is d = 16.29 Å. Hence, the Bohr radius of P-donor in such a system is ∼16.29 Å, which is far smaller than the bulk case (∼25 Å).[31] The reduction in the Bohr radius happens due to the quantum confinement effect. We study the PDOS spectra of N-donor in H:SiNW as shown in Figs. 3(e)–3(h) and find a similar trend of features as we shift far from the donor location. The PDOS for A_1 state reduces to a negligible value at d = 5.43 Å, which signifies the ground state is highly concentrated and the Bohr radius is ∼5.43 Å.

We also observe that A_1 state is largely separated from any other states of this configuration. The difference between N-donor's ground state and the first excited state (ES) is 770 meV, while that for P-donor is 118 meV. This is consistent with the highly localized ground state of N-donor. Such a highly localized and deep ground state is the pathway for designing quantum devices for room temperature.

To calculate the binding energy of the donor electron (E_b), we estimated the lowest effective conductive state of doped H:SiNW following Anh *et al.*[33] Since the donor electronic states hybridize with silicon electronic states, the conductive state changes in comparison with the undoped system. The E_b is estimated by taking the ratio of PDOS/TDOS, which signifies the relative weight of donor states against the states of the whole system. Figures 4(a) and 4(b) show the PDOS/TDOS spectra for P-donor and N-donor, respectively. At the lower energy range, the contribution of the donor is dominated, while the contribution is trivial at higher energy range (above the blue dashed line) due to the inclusion of more number of silicon atoms. The binding energy is calculated from the point where this ratio saturates close to 0. The calculated E_b values for P-donor and N-donor are 1.36 and 2.40 eV, respectively.

In order to understand the behavior of undoped and doped devices, LDOS spectra are simulated along with the current vs gate voltage (I_{DS}–V_G) characteristics for different source to drain voltage (V_{DS}) using the transistor device parameters described in Fig. 1(c). The LDOS spectrum of the undoped H:SiNW transistor is obtained where no states are observed below the conduction band edge as shown in Fig. 5(a). In Figs. 5(b) and 5(c), extra energy states are observed in the LDOS data due to substitutionally doped P-donor and N-donor, respectively.

The lowest energy state in the channel region of the P-doped device is found at 80 meV from the next conductive state, which is low compared to non-device configuration (118 meV). This is most likely due to the effect of metal gate and closely spaced heavily doped leads. In the LDOS graph of the N-doped device, a very deep energy state is observed at 322 meV below the nearest conductive state. To look into the fine features of these configurations, the LDOS spectra of all these systems are mapped along the vertical axis in Figs. 5(d)–5(f). The LDOS spectra along the Z axis at z = 26.93 Å are presented for all three device structures. We do not observe any state below CBE for the undoped device as shown in Fig. 5(d). A single LDOS peak in P-doped SiNW at 80 meV is observed in Fig. 5(e), indicating the GS of P-donor in the device configuration. A highly localized LDOS is also perceived at 322 meV from the CBE in Fig. 5(f), providing the information of the GS of N-dopant in the device configuration. In addition, we also observed first ES of the N-donor at 54 meV below the CBE.

The I_{DS}–V_G transport characteristics for all three devices are simulated at different bias voltages for T = 5 and 300 K, as presented in Figs. 5(g)–5(k). In the undoped device with $V_{DS} = 5$ mV, the characteristics are typical FET devices, which is consistent with the LDOS spectrum of this device configuration. The weak modulation in I_{DS} for T = 5 K is observed at $V_G \approx 0.5$ mV in Fig. 5(g), which is due to the transport through the discrete states in the conduction band (CB) of the undoped H:SiNW. It is also observed that the subthreshold slopes of I_{DS}–V_G curves at 5 and 300 K are almost same, which may be due to the effect of heavy doping (10^{21} cm^{-3}) of the leads along with the nano-channel effect.

The transport characteristics for the P-doped device are presented in Figs. 5(h) and 5(i) for $V_{DS} = 1$ and 5 mV, respectively, showing a strong single-electron tunneling current peak before the onset of FET current at T = 5 K due to the existence of the localized state of the P-donor within the channel window. An additional weak current peak is also preserved due to the transport through the next discrete conducting state. However, this SET peak dies out at 300 K due to the shallow nature of such dopant.

The I_{DS}–V_G characteristics for the N-doped device are presented in Figs. 5(j) and 5(k) for $V_{DS} = 1$ and 5 mV, respectively. For $V_{DS} = 1$ mV, a very strong tunneling peak is observed via the GS of N-donor. However, the GS and first ES prominently participated in the transport characteristics at T = 300 K. The excited state features are observed at high temperature due to higher tunnel rate compared to 5 K. For $V_{DS} = 5$ mV and T = 5 K, the low temperature behavior of the device is similar to $V_{DS} = 1$ mV with lower separation from the FET current, and this current peak is also strongly sustained at T = 300 K. Along with the transport through the GS at 300 K, a small hump corresponding to first excited state is also noted. A single-electron current peak at room temperature is observed due to the deep nature of the N-donor. Such a deep donor state is capable of holding the quantum information and is less fragile to the environmental fluctuations compared to the shallow donor. Since silicon is one of the most promising semiconductor for quantum information devices due to large charge and spin coherence times,[34–37] the donor state of nitrogen in silicon gives an opportunity to utilize it for better performances. Hence, to design a single-electron transistor with a single donor atom for room-temperature operation, N-donor in silicon could be one of the best systems. We are working in such a direction for the experimental realization of the room-temperature SET devices.

The donor energy spectrum of nitrogen in hydrogenated-silicon nanowire is theoretically investigated in comparison with phosphorous and undoped systems. We observed that the binding energy of N-donor ground state is large compared to the P-donor. The N-donor

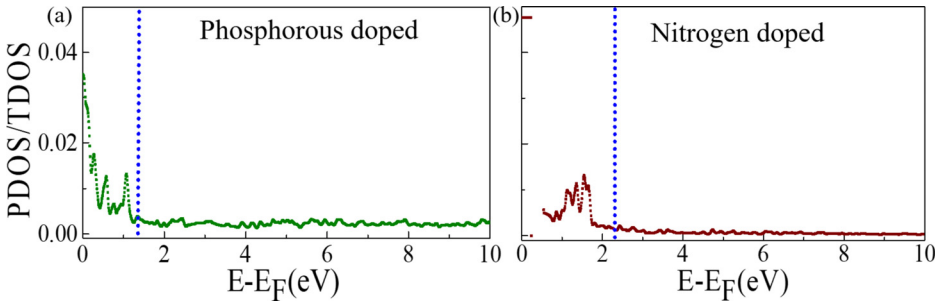

FIG. 4. (a) and (b) PDOS/TDOS spectra of a P-doped and a N-doped silicon nanowire, respectively.

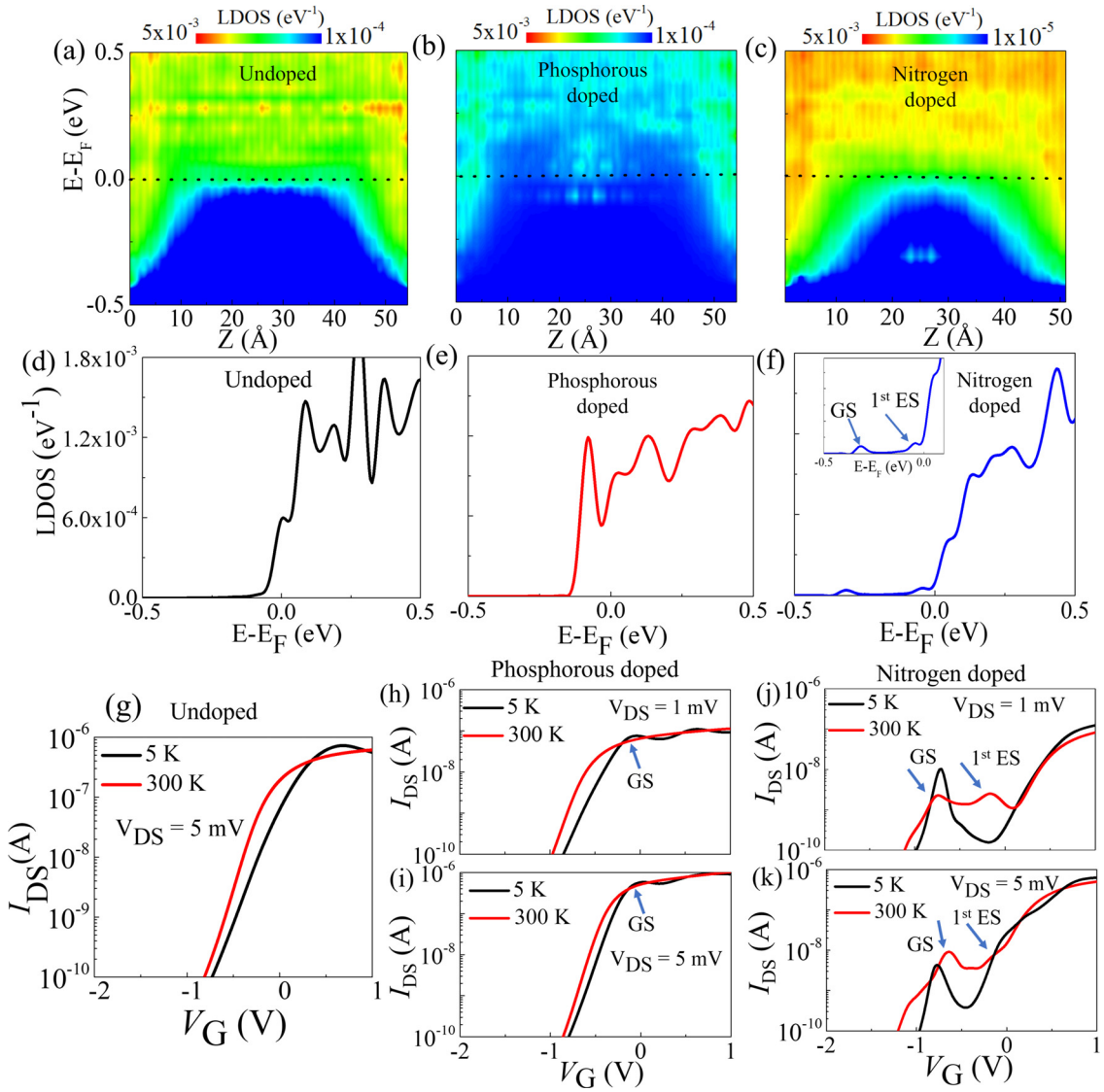

FIG. 5. (a)–(c) LDOS spectra of an undoped, P-doped, and N-doped silicon nanowire transistors, respectively. (d)–(f) LDOS spectra at z = 26.93 Å for undoped, P-doped, and N-doped silicon nanowire transistor, respectively. Inset of Fig. 5(f) indicates the zoom in spectrum, exhibiting the GS and first ES of N-donor. Simulated I_{DS}–V_G characteristics for (g) undoped, (h) and (i) P-doped, and (j) and (k) N-doped devices.

is highly localized, and separation of the ground state is also very large compared to the first excited state. In quantum devices where perseverance of quantum states is important, this advantage can be taken from a natural system with deep N-donor state. Simulated LDOS and I_{DS}–V_G characteristics of the devices also suggest in favor of N-dopant as the potential candidate for single-electron tunneling devices for room-temperature operation, which further reinforces that this system could be useful for designing practical quantum architecture.

The authors are thankful to Professor Sparsh Mittal for the computational resources under the Project No. ECR/2017/000622. The authors also thank to Professor Sanjeev Manhas for computational support under MIT-896-ECD EICT Academy IIT Roorkee. This work was partially supported by DST-SERB (Project No. ECR/2017/001050) and IIT Roorkee (Project No. FIG-100778-PHY), India. P.Y. and H.A. thank the Ministry of Education and UGC, India, respectively, for the research scholarship.

AUTHOR DECLARATIONS

Conflict of Interest

The authors have no conflicts to disclose.

Author Contributions

Pooja Yadav: Conceptualization (equal); Data curation (equal); Formal analysis (equal); Investigation (equal); Methodology (equal); Validation

(equal); Visualization (equal); Writing – original draft (equal). **Hemant Arora:** Conceptualization (equal); Data curation (equal); Formal analysis (equal); Investigation (equal); Methodology (equal); Writing – original draft (equal). **Arup Samanta:** Conceptualization (equal); Formal analysis (equal); Funding acquisition (equal); Investigation (equal); Methodology (equal); Project administration (equal); Resources (equal); Software (equal); Supervision (equal); Validation (equal); Visualization (equal); Writing – review & editing (equal).

DATA AVAILABILITY

The data that support the findings of this study are available within the article.

REFERENCES

[1]B. E. Kane, Nature **393**, 133 (1998).
[2]R. Vrijen, E. Yablonovitch, K. Wang, H. W. Jiang, A. Balandin, V. Roychowdhury, T. Mor, and D. DiVincenzo, Phys. Rev. A **62**, 012306 (2000).
[3]L. C. L. Hollenberg, A. D. Greentree, A. G. Fowler, and C. J. Wellard, Phys. Rev. B **74**, 045311 (2006).
[4]L. C. L. Hollenberg, A. S. Dzurak, C. Wellard, A. R. Hamilton, D. J. Reilly, G. J. Milburn, and R. G. Clark, Phys. Rev. B **69**, 113301 (2004).
[5]L. Guo, E. Leobandung, and S. Y. Chou, Appl. Phys. Lett. **70**, 850 (1997).
[6]G. P. Lansbergen, Y. Ono, and A. Fujiwara, Nano Lett. **12**, 763 (2012).
[7]X. Wang, S. Huang, J. Y. Wang, D. Pan, J. Zhao, and H. Q. Xu, Nanoscale **13**, 1048 (2021).
[8]O. Astafiev, V. Antonov, T. Kutsuwa, and S. Komiyama, Nature **403**, 405 (2000).
[9]M. Tabe, D. Moraru, M. Ligowski, M. Anwar, R. Jablonski, Y. Ono, and T. Mizuno, Phys. Rev. Lett. **105**, 016803 (2010).
[10]H. Sellier, G. P. Lansbergen, J. Caro, S. Rogge, N. Collaert, I. Ferain, M. Jurczak, and S. Biesemans, Phys. Rev. Lett. **97**, 206805 (2006).
[11]Y. Ono, M. A. H. Khalafalla, K. Nishiguchi, K. Takashina, A. Fujiwara, S. Horiguchi, H. Inokawa, and Y. Takahashi, Appl. Surf. Sci. **254**, 6252 (2008).
[12]E. Prati, M. Hori, F. Guagliardo, G. Ferrari, and T. Shinada, Nat. Nanotechnol. **7**, 443 (2012).
[13]M. Fuechsle, J. A. Miwa, S. Mahapatra, H. Ryu, S. Lee, O. Warschkow, L. C. L. Hollenberg, G. Klimeck, and M. Y. Simmons, Nat. Nanotechnol. **7**, 242 (2012).
[14]M. Pierre, R. Wacquez, X. Jehl, M. Sanquer, M. Vinet, and O. Cueto, Nat. Nanotechnol. **5**, 133 (2010).
[15]A. Samanta, M. Muruganathan, M. Hori, Y. Ono, H. Mizuta, M. Tabe, and D. Moraru, Appl. Phys. Lett. **110**, 093107 (2017).
[16]E. Hamid, D. Moraru, Y. Kuzuya, T. Mizuno, L. T. Anh, H. Mizuta, and M. Tabe, Phys. Rev. B **87**, 085420 (2013).
[17]M. J. Calderón, B. Koiller, and S. D. Sarma, Phys. Rev. B **75**, 125311 (2007).
[18]R. Lo Nardo, G. Wolfowicz, S. Simmons, A. M. Tyryshkin, H. Riemann, N. V. Abrosimov, P. Becker, H. J. Pohl, M. Steger, S. A. Lyon, M. L. W. Thewalt, and J. J. L. Morton, Phys. Rev. B. **92**, 165201 (2015).
[19]C. Yin, M. Rancic, G. G. De Boo, N. Stavrias, J. C. McCallum, M. J. Sellars, and S. Rogge, Nature **497**, 91–94 (2013).
[20]S. Achilli, N. H. Le, G. Fratesi, N. Manini, G. Onida, M. Turchetti, G. Ferrari, T. Shinada, T. Tanii, and E. Prati, Adv. Funct. Mater. **31**, 2011175 (2021).
[21]S. Achilli, N. Manini, G. Onida, T. Shinada, T. Tanii, and E. Prati, Sci. Rep. **8**, 18054 (2018).
[22]K. Ono, T. Mori, and S. Moriyama, Sci. Rep. **9**, 469 (2019).
[23]K. K. Ng and S. M. Sze, *Physics of Semiconductor Devices Physics of Semiconductor Devices,* 3rd ed. (John Wiley and Sons, 1995).
[24]A. M. Tyryshkin, S. Tojo, J. J. L. Morton, H. Riemann, N. V. Abrosimov, P. Becker, H. J. Pohl, T. Schenkel, M. L. W. Thewalt, K. M. Itoh, and S. A. Lyon, Nat. Mater. **11**, 143 (2012).
[25]S. Smidstrup, T. Markussen, P. Vancraeyveld, J. Wellendorff, J. Schneider, T. Gunst, B. Verstichel, D. Stradi, P. A. Khomyakov, U. G. Vej-Hansen, M. E. Lee, S. T. Chill, F. Rasmussen, G. Penazzi, F. Corsetti, A. Ojanperä, K. Jensen, M. L. N. Palsgaard, U. Martinez, A. Blom, M. Brandbyge, and K. Stokbro, J. Phys.: Condens. Matter **32**, 015901 (2020).
[26]K. Stokbro, D. E. Petersen, S. Smidstrup, A. Blom, M. Ipsen, and K. Kaasbjerg, Phys. Rev. B **82**, 075420 (2010).
[27]G. Makov, R. Shah, and M. Payne, Phys. Rev. B **53**, 15513 (1996).
[28]H. Haug and A.-P. Jauho, *Quantum kinetics in transport and optics of semiconductors* (Springer, 2008).
[29]"Group IV elements, IV-IV and III-V compounds. Part b—Electronic, transport, optical and other properties," in *Numerical Data and Functional Relationships in Science and Technology*, Landolt-Börnstein, New Series, Group III Vol. 22, edited by O. Madelung, U. Rössler, and M. Schulz (Springer, Berlin, 1982).
[30]B. Guan, H. Siampour, Z. Fan, S. Wang, X. Y. Kong, A. Mesli, J. Zhang, and Y. Dan, Sci. Rep. **5**, 12641 (2015).
[31]W. Kohn and J. M. Luttinger, Phys. Rev. **98**, 915 (1955).
[32]A. L. Saraiva, A. Baena, M. J. CalderÓn, and B. Koiller, J. Phys.: Condens. Matter **27**, 154208 (2015).
[33]L. The Anh, D. Moraru, M. Manoharan, M. Tabe, and H. Mizuta, J. Appl. Phys. **116**, 063705 (2014).
[34]Z. Zhou, M. L. Steigerwald, R. A. Friesner, L. Brus, and M. S. Hybertsen, Phys. Rev. B **71**, 245308 (2005).
[35]F. A. Zwanenburg, A. S. Dzurak, A. Morello, M. Y. Simmons, L. C. L. Hollenberg, G. Klimeck, S. Rogge, S. N. Coppersmith, and M. A. Eriksson, Rev. Mod. Phys. **85**, 961 (2013).
[36]M. Tyryshkin, A. Lyon, V. Astashkin, and M. Raitsimring, Phys. Rev. B. **68**, 193207 (2003).
[37]M. Steger, K. Saeedi, M. L. W. Thewalt, J. J. L. Morton, H. Riemann, N. V. Abrosimov, P. Becker, and H.-J. Pohl, Science **336**, 1280 (2012).